Elastic Properties and Polymorphic Behavior of Fibers of Syndiotactic Polypropylene at Different Temperatures

Claudio De Rosa,*,† Maria Carla Gargiulo,† Finizia Auriemma,† Odda Ruiz de Ballesteros,† and Abbas Razavi‡

Dipartimento di Chimica, Università di Napoli "Federico II", Complesso Monte S.Angelo, Via Cintia, 80126 Napoli, Italy, and ATOFINA Petrochemicals Inc., Research and Technology Center, 1700 Battle Ground Road, La Porte, Texas 77571

Received March 15, 2002; Revised Manuscript Received July 19, 2002

ABSTRACT: An analysis of the elastic properties of syndiotactic polypropylene at different temperatures is reported. Fibers stretched at low temperatures are in the *trans*-planar form III, which transforms into the helical form II upon the release of the tension, whereas fibers stretched at high temperatures are in the stable helical form I. The mechanical analysis of these fibers has shown that only at room temperatures the specimens show good elastic properties. The elastic recovery of the samples is in part lost also at room temperature in annealed fibers, which are in the stable form I, in both the stretched and unstrained states. When the structural transition from the *trans*-planar form III into the helical form occurs upon removing the tension, a nearly total elastic recovery is observed. Only a partial elastic recovery is instead observed when this transition is absent. The relative amount of crystalline phase in unoriented films and in stretched and stress-relaxed fibers is rather constant (≈40−43%) and does not depend on the stretching temperature in the range 25−80 °C. These data indicate that the elastic behavior of syndiotactic polypropylene is in part linked to the enthalpy gain achieved when the tension is removed, due to the metastability, in the unstrained state, of the *trans*-planar form, which transforms into the stable helical form. On the other hand, also an entropic factor must play a role, due to the entangled amorphous chains which experience a reversible conformational transition between the disordered (coil) and extended conformations during the stretching and relaxing process.

Introduction

Syndiotactic polypropylene (s-PP) presents a very complex polymorphic behavior.[1−14] Four crystalline forms, shown in Figure 1, have been described so far. The most stable form I (Figure 1A) and the metastable form II (Figure 1B) are characterized by chains in s(2/1)2 helical $(T_2G_2)_n$ conformation, packed in orthorhombic unit cells.[2,4]

The two metastable modifications, form III (Figure 1C) and form IV (Figure 1D), present chains in *trans*-planar[3,8] and $(T_6G_2T_2G_2)_n$[9] helical conformations, respectively, and can be obtained only in oriented fibers. The *trans*-planar form III has been, indeed, obtained by cold drawing procedures of low stereoregular s-PP samples[3] or by stretching at room temperature highly stereoregular samples prepared with metallocene catalysts.[8] Form IV is instead obtained by exposing fiber samples initially in form III to vapors of various solvents (e.g., benzene, toluene).[9]

The formation of the four crystalline modifications depends on the condition of crystallization and the stereoregularity of the polymer sample.[10] Form I is considered to be the thermodynamically stable form of s-PP obtained under the most common conditions of crystallization, from the melt and/or precipitation from solution, in powder samples and single crystals of s-PP.[4−7,11] In the limit ordered model of form I (Figure 1A) right- and left-handed helices alternate along both axes of the unit cell, whereas disorder in this alternation is present in samples crystallized from the melt at low temperatures[11] or single crystals grown at low temperatures.[7]

Form II is characterized by a C-centered structure where 2-fold helical chains having the same chirality are included in the orthorhombic unit cell (Figure 1B).[2] It is a metastable polymorph of s-PP and has been obtained only in oriented fibers of s-PP[2,10,12,13] and, recently, by melt-crystallization at elevated pressure.[14] It has been, indeed, obtained by stretching at room temperature compression-molded specimens of low stereoregular s-PP samples prepared with vanadium-based Ziegler−Natta catalysts[2,10,12,13] or upon releasing the tension in stretched fibers of highly stereoregular s-PP samples initially in form III.[12] In fact, when highly stereoregular samples, prepared with homogeneous metallocene catalysts, are stretched at room temperature, the *trans*-planar form III is obtained, which transforms into the isochiral helical form II by releasing the tension.[12,13] In powder unoriented s-PP samples only disordered modifications of form II, characterized by conformationally disordered chains containing *trans*-planar sequences (kink bands defects),[15] can be obtained at atmospheric pressure, for instance, by precipitation from solutions of low stereoregular samples[15] and in copolymers of s-PP with ethylene comonomeric units.[16−18]

The metastable polymorphic forms II, III, and IV generally transform into the stable form I by annealing.[10]

The complex polymorphic behavior of s-PP influences its macroscopic properties. For instance, oriented fibers of s-PP show an elastic behavior which is related to the structural organization. Unoriented compression-molded samples of s-PP behave like a typical highly crystalline material showing a plastic deformation upon stretching at room temperature.[13,19,20] The crystalline domains, with chains in helical conformation, tend to assume a preferred orientation along the stretching direction

† Università di Napoli "Federico II".
‡ ATOFINA Petrochemicals Inc.

10.1021/ma020394+ CCC: $22.00
Published on Web 10/16/2002

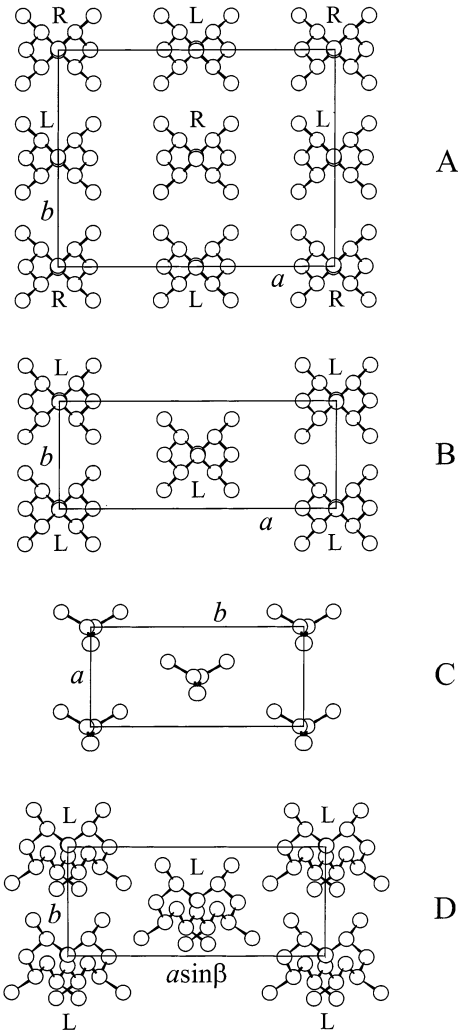

Figure 1. Models of packing of the limit ordered form I (a = 14.5 Å, b = 11.2 Å, c = 7.4 Å) (A), form II (a = 14.5 Å, b = 5.6 Å, c = 7.4 Å) (B), form III (a = 5.22 Å, b = 11.17 Å, c = 5.06 Å) (C), and form IV (a = 14.17 Å, b = 5.72 Å, c = 11.6 Å, β = 108.8°) (D) of s-PP. R = right-handed helix; L = left-handed helix.

originating a plastic, not reversible, deformation. High orientation of the crystalline phase is generally achieved. Along with this plastic deformation, a phase transition from the most stable helical form into the form III with chains in the *trans*-planar conformation gradually occurs. The phase transition is reversible; after the release of the tension the crystalline domains remain nearly oriented with the *c* axis parallel to the preferred (stretching) direction, and the *trans*-planar form III transforms again into the more stable helical form. As a result, for not previously oriented material, a partial recovery of the macroscopic dimensions of the sample is attained. Therefore, unoriented samples show only fair or poor elastic properties.[13,19,20] Stress-relaxed fibers show instead very good elastic behavior upon successive stretching and relaxation; the helical form transforms by stretching into the *trans*-planar form, which transforms again into the helical form by releasing the tension, and a nearly total recovery of the initial dimensions of the fiber samples is observed.[13] When the crystalline domains are already oriented along the stretching direction, that is, when the sample has already undergone the plastic deformation, the fibers show good elastic properties.[13,19,20] Of course, during the mechanical cycles also the chains in the amorphous regions are subjected to a reversible conformational transition, from the "random coils" into extended conformations, and vice versa. This reversibility of the transition is possibly assisted and is, somehow, favored by the polymorphic transition occurring in the crystalline regions.

It has been suggested that while the driving force which induces the recovery of the initial dimensions in common elastomers upon the release of the stress is mainly entropic, in the case of s-PP it is basically linked to the enthalpy gain achieved when the sample is relaxed due to the metastability of the *trans*-planar form III.[13] On the other hand, it has been also hypothesized that the elastic behavior is mainly due to the conformational transition occurring in the amorphous phase for chains connecting the crystalline domains.[19,20]

The studies of the mechanical properties of s-PP have shown that fibers samples behave as thermoplastic elastomer having high modulus (≈300 MPa). It may be of interest to analyze whether these outstanding properties are maintained at temperatures higher than room temperature, because in these conditions the properties of other thermoplastic elastomers generally fail. Studies of the elastic properties of s-PP at high temperatures have not been reported so far. In this paper, the polymorphic behavior of s-PP fibers and the corresponding mechanical properties have been analyzed at different temperatures, also to give new insights into the relationships between the elastic behavior and the structural organization of s-PP. Since it is expected that the temperature influences the polymorphic behavior of s-PP, the measurement of the mechanical properties at different temperatures may clarify the reciprocal roles played by the polymer chains in the crystalline and amorphous phases in the elastic recovery of s-PP.

Experimental Section

The s-PP sample was prepared in the laboratories of ATOFINA Petrochemicals Research by using homogeneous metallocene-based catalytic system. The molecular weight of the sample is $M_w = 1.93 \times 10^5$ with polydispersity M_w/M_n = 4.5. The microstructure of the polymer chains, determined by the solution ^{13}C NMR spectrum, is characterized by a fraction of the fully syndiotactic pentad [*rrrr*] of 78%, with a random distribution of defects of stereoregularity (mainly *mm* triads and *m* dyads) and the absence of defects of regioregularity.

Compression-molded films used for the measurements of the mechanical properties and the preparation of oriented fibers were obtained by melting the s-PP powder sample at 150 °C between perfectly flat brass plates under a press at very low pressure and slowly cooling to room temperature. Special care has been taken to obtain films with uniform thickness (0.3 mm) and minimize surface roughness, according to the recommendation of the standard ASTM D-2292-85. X-ray diffraction profiles indicate that these films are crystallized in the stable form I,[4] with a crystallinity of nearly 40%.

The mechanical tests were performed at various temperatures with a miniature mechanical tester apparatus (Minimat, by Rheometrics Scientific), following the standard test method for tensile properties of thin plastic sheeting ASTM D882-83.

The experiments performed in this paper on unoriented compression-molded films and oriented fibers of s-PP are reported in Table 1. The mechanical tests were first performed at different temperatures on the unstretched compression-molded films. Rectangular specimens 10 mm long, 5 mm wide, and 0.3 mm thick were stretched at temperatures of 25, 40, 60, and 80 °C up to the break (experiments 1−4 in Table 1) or up to a given strain ϵ (experiments 1a−4a in Table 1).

Table 1. Description of the Experiments of Stretching on Unoriented Compression-Molded Films and Oriented Fibers of s-PP[a]

expt	starting material	description	initial length	final length	deformation ϵ (%)	sample obtained
1	unoriented film	stretching at 25 °C	L_0	break	1335	
1a	unoriented film	stretching at 25 °C	L_0	$L_f = 7L_0$	600	fiber sPP1
1b	fiber sPP1	removing the tension	L_f	L_r	residual deformation: $100(L_r - L_0)/L_0 = 314\%$	stress-relaxed fiber sPP25
1c	fiber sPP25	stretching at 25 °C	L_r	break	94	
1d	fiber sPP25	stretching at 25 °C	L_r	$L_f = 7L_0$	$100(L_f - L_r)/L_r$	fiber sPP25st
1e	fiber sPP25st	removing the tension	L_f	L_r'	residual deformation: $100(L_r' - L_r)/L_r = 8\%$	
2	unoriented film	stretching at 40 °C	L_0	break	1538	
2a	unoriented film	stretching at 40 °C	L_0	$L_f = 7L_0$	600	fiber sPP2
2b	fiber sPP2	removing the tension	L_f	L_r	residual deformation: $100(L_r - L_0)/L_0 = 355\%$	stress-relaxed fiber sPP40
2c	fiber sPP40	stretching at 25 °C	L_r	break	81	
2d	fiber sPP40	stretching at 25 °C	L_r	$L_f = 7L_0$	$100(L_f - L_r)/L_r$	fiber sPP40st
2e	fiber sPP40st	removing the tension	L_f	L_r'	residual deformation: $100(L_r' - L_r)/L_r = 8\%$	
3	unoriented film	stretching at 60 °C	L_0	break	1380	
3a	unoriented film	stretching at 60 °C	L_0	$L_f = 7L_0$	600	fiber sPP3
3b	fiber sPP3	removing the tension	L_f	L_r	residual deformation: $100(L_r - L_0)/L_0 = 380\%$	stress-relaxed fiber sPP60
3c	fiber sPP60	stretching at 25 °C	L_r	break	68	
3d	fiber sPP60	stretching at 25 °C	L_r	$L_f = 7L_0$	$100(L_f - L_r)/L_r$	fiber sPP60st
3e	fiber sPP60st	removing the tension	L_f	L_r'	residual deformation: $100(L_r' - L_r)/L_r = 4\%$	
4	unoriented film	stretching at 80 °C	L_0	break	1446	
4a	unoriented film	stretching at 80 °C	L_0	$L_f = 7L_0$	600	fiber sPP4
4b	fiber sPP4	removing the tension	L_f	L_r	residual deformation: $100(L_r - L_0)/L_0 = 527\%$	stress-relaxed fiber sPP80
4c	fiber sPP80	stretching at 25 °C	L_r	break	36	
4d	fiber sPP80	stretching at 25 °C	L_r	$L_f = 7L_0$	$100(L_f - L_r)/L_r$	fiber sPP80st
4e	fiber sPP80st	removing the tension	L_f	L_r'	residual deformation: $100(L_r' - L_r)/L_r = -$	
5	fiber sPP25	hysteresis at 60 °C	L_r	$L_f = 7L_0$	$100(L_f - L_r)/L_r$	
6	fiber sPP25	hysteresis at 80 °C	L_r	$L_f = 7L_0$	$100(L_f - L_r)/L_r$	
7	fiber sPP25st	annealing at 95 °C	$L_f = 7L_0$			fiber sPP25a
7a	fiber sPP25a	removing the tension	$L_f = 7L_0$	L_{ra}	residual deformation: $100(L_{ra} - L_r)/L_r = 31\%$	fiber sPP25ar
7b	fiber sPP25ar	stretching at 25 °C	L_{ra}	$L_f = 9L_0$	$100(L_f - L_{ra})/L_{ra}$	fiber sPP25arst
7c	fiber sPP25arst	removing the tension	$L_f = 9L_0$	L_{ra}	residual deformation: $100(L_{ra} - L_{ra})/L_{ra} = 0$	

[a] The initial and final lengths in each experiment and the corresponding deformation of the sample are indicated.

The mechanical tests were then performed at room temperature on the strained and stress-relaxed fibers. The stress-relaxed fiber specimens, prepared by stretching the compression molded films at 25, 40, 60, and 80 °C (experiments 1a-4a in Table 1), and then removing the tension (experiments 1b-4b in Table 1), have been identified as samples sPP25, sPP40, sPP60 and sPP80, respectively (Table 1). Compression molded films stretched at the different temperatures (experiments 1a-4a in Table 1) were kept under tension for 2 days at room temperature, then the tension was removed allowing the specimens to relax (experiments 1b-4b in Table 1). These stress-relaxed fibers were stretched again at room temperature up to the break (experiments 1c-4c in Table 1), or up to a given elongation ϵ (experiments 1d−4d in Table 1).

In the mechanical tests the free gauge length was 10 mm, and the ratio between the drawing rate and the initial length was fixed equal to 0.1 mm/(mm min) for the measurement of Young's modulus and 1 mm/(mm min) for the measurement of stress−strain curves and the determination of the other mechanical properties (stress and strain at break, tension set). The values of the tension set were measured according to the standard test method ASTM D412-87. The specimens of initial length L_0 were stretched up to a length L_f, i.e., up to the elongation $\epsilon = [(L_f - L_0)/L_0] \times 100$, and held at this elongation for 2 days, then the tension was removed, and the final length of the relaxed specimens L_r was measured after 10 min (for instance, experiments 1a, 1b, or 1d, 1e in Table 1). The tension set was calculated by using the following formula: $t_s(\epsilon) = [(L_r - L_0)/L_0] \times 100$, whereas the elastic recovery was calculated as $r(\epsilon) = [(L_f - L_r)/L_r] \times 100$. The reported values of the mechanical properties are averaged over at least five independent experiments.

The X-ray fiber diffraction patterns were obtained with Cu Kα radiation and recorded on a BAS-MS imaging plate (FUJIFILM) using a cylindrical camera and processed with a digital imaging reader (FUJIBAS 1800). The X-ray patterns have been recorded for stretched fibers soon after the stretching and keeping the fiber under tension and for relaxed fibers, that is, after keeping the fiber under tension for 2 days and then removing the tension allowing the complete relaxation of the specimens.

The degrees of orientation of stretched and stress-relaxed fibers have been evaluated from the X-ray fiber diffraction patterns as the half-height width of the peaks obtained in the azimuthal scans of the reflections having the strongest intensity.

The degrees of crystallinity of oriented sPP fibers have been evaluated from the 2D X-ray fiber diffraction patterns. From these patterns, monodimensional X-ray intensity profiles as a function of 2θ have been obtained integrating the intensity along the azimuthal angle with constant value of 2θ, at interval of $\Delta 2\theta = 0.4°$, in the 2θ range 10°−30°. The diffraction profile of the amorphous phase has been evaluated, performing the same procedure, from the 2D X-ray diffraction pattern of a sample of atactic polypropylene, obtained with the same cylindrical camera. The amorphous profile was then scaled and subtracted from the X-ray diffraction profiles of the crystalline fibers. The degree of crystallinity was therefore calculated from the ratio of the so-obtained crystalline diffracting area and the total area of the X-ray diffraction profiles.

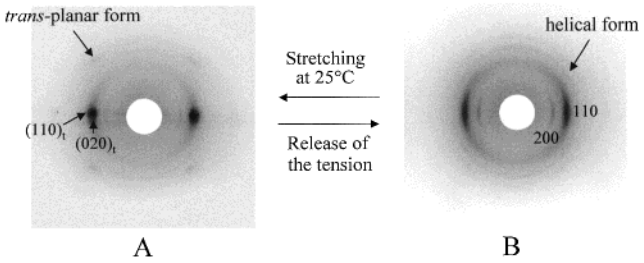

Figure 2. X-ray fiber diffraction patterns, recorded at room temperature, of s-PP fibers obtained by stretching at 25 °C compression-molded films at 600% elongation (experiment 1a in Table 1), keeping the fiber under tension (A) and after the release of the tension (experiment 1b in Table 1) (B). The $(020)_t$ and $(110)_t$ reflections of the *trans*-planar form III and the 200 and 110 reflections of the helical form II are indicated. On the first layer line, the reflections arising from the diffraction of crystals in the *trans*-planar form III with a periodicity of 5.1 Å (021 reflection) and in the helical form with a periodicity of 7.4 Å (111 reflection) are also indicated. The fiber in (A) is basically in the *trans*-planar form III, whereas the fiber in (B) is in the helical form II.

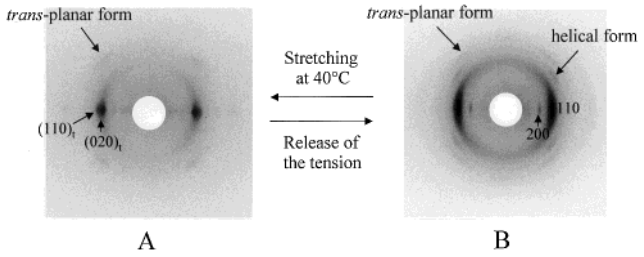

Figure 3. X-ray fiber diffraction patterns, recorded at room temperature, of s-PP fibers obtained by stretching at 40 °C compression-molded films at 600% elongation (experiment 2a in Table 1), keeping the fiber under tension (A) and after the release of the tension (experiment 2b in Table 1) (B). The $(020)_t$ and $(110)_t$ reflections of the *trans*-planar form III and the 200 and 110 reflections of the helical form II are indicated. On the first layer line, the reflections arising from the diffraction of crystals in the *trans*-planar form III with a periodicity of 5.1 Å (021 reflection) and in the helical form with a periodicity of 7.4 Å (111 reflection) are also indicated. The fiber in (A) is basically in the *trans*-planar form III, whereas the fiber in (B) is in a mixture of the helical form II and ordered domains with chains in *trans*-planar conformation.

Results and Discussion

Polymorphic Behavior. The X-ray fiber diffraction patterns of oriented fibers of s-PP, obtained by stretching compression-molded films at 600% elongation at 25, 40, 60, and 80 °C, and keeping the fibers under tension at room temperature (experiments 1a−4a of Table 1), are reported in parts A of Figures 2, 3, 4, and 5, respectively. The patterns of the stress-relaxed fibers, after the release of the tension and allowing complete relaxation of the fibers (experiments 1b−4b), are shown in parts B of the same figures. The corresponding X-ray diffraction profiles read along the equatorial lines are reported in the Figures 6 and 7 for the strained and stress-relaxed fibers, respectively. Since the compression-molded film already presents high crystallinity (about 40%), because of the slow crystallization from the melt (see experimental part), the crystallinities of the fiber samples stretched at different temperatures are similar and do not increase significantly because of the annealing at high temperature. The degrees of crystallinity of the fibers stretched at 25, 40, 60, and 80 °C, evaluated from the patterns of Figures 2−5, are, indeed, 40, 42, 42, and 43%, respectively. The same values of

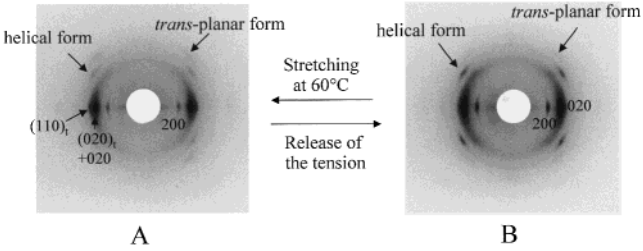

Figure 4. X-ray fiber diffraction patterns, recorded at room temperature, of s-PP fibers obtained by stretching at 60 °C compression-molded films at 600% elongation (experiment 3a in Table 1), keeping the fiber under tension (A) and after the release of the tension (experiment 3b in Table 1) (B). The $(020)_t$ and $(110)_t$ reflections of the *trans*-planar form III and the 200 and 020 reflections of the helical form I are indicated. On the first layer line, the reflections arising from the diffraction of crystals in the *trans*-planar form III with a periodicity of 5.1 Å (021 reflection) and in the helical form with a periodicity of 7.4 Å (111 reflection) are also indicated. The fiber in (A) is in a mixture of the *trans*-planar form III and the helical form I, whereas the fiber in (B) is basically in the helical form I with a small amount of ordered domains with chains in *trans*-planar conformation.

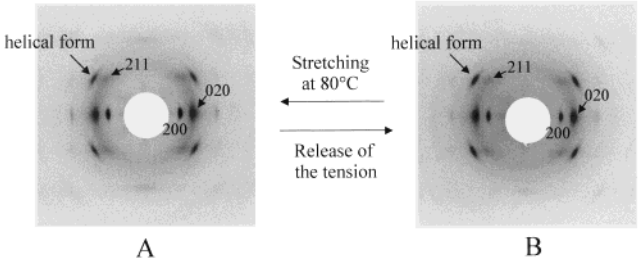

Figure 5. X-ray fiber diffraction patterns, recorded at room temperature, of s-PP fibers obtained by stretching at 80 °C compression-molded films at 600% elongation (experiment 4a in Table 1), keeping the fiber under tension (A) and after the release of the tension (experiment 4b in Table 1) (B). The 200, 020, and 211 reflections of the helical form I are indicated. On the first layer line, the 111 reflection arising from the diffraction of crystals in the helical form with a periodicity of 7.4 Å is also indicated. Both fibers in (A) and (B) are in the pure helical form I.

crystallinity are observed upon releasing the tension (Figures 2B−5B). It is apparent form Figures 2A and 3A that at low temperatures (25 and 40 °C) the *trans*-planar form III is obtained by stretching, as indicated by the presence of the equatorial $(020)_t$ e $(110)_t$ reflections at $2\theta = 15.9°$ and 18.8°, respectively (Figure 6, A and B), typical of form III, and spots on the first layer line corresponding to a chain periodicity of $c = 5.1$ Å. Small bumps at $2\theta = 12.2°$, corresponding to the 200 reflection, are also present in the patterns of Figure 6A,B, indicating that a negligible amount of crystals of helical form is also present.

With increasing the stretching temperature a mixture of the *trans*-planar form III and the crystalline modification of s-PP with chains in helical conformation is obtained by stretching. For instance, the X-ray diffraction pattern of the fiber stretched at 60 °C (Figures 4A and 6C) shows, besides the reflections of form III, also the equatorial 200 refection at $2\theta = 12.2°$ (Figure 6C), typical of the helical forms (forms I or II) of s-PP, and spots on the layer lines corresponding to both chain periodicities of $c = 5.1$ Å (*trans*-planar) and $c = 7.4$ Å (2-fold helical) (Figure 4A).

At higher stretching temperatures only the helical form I is obtained. For instance, the X-ray diffraction

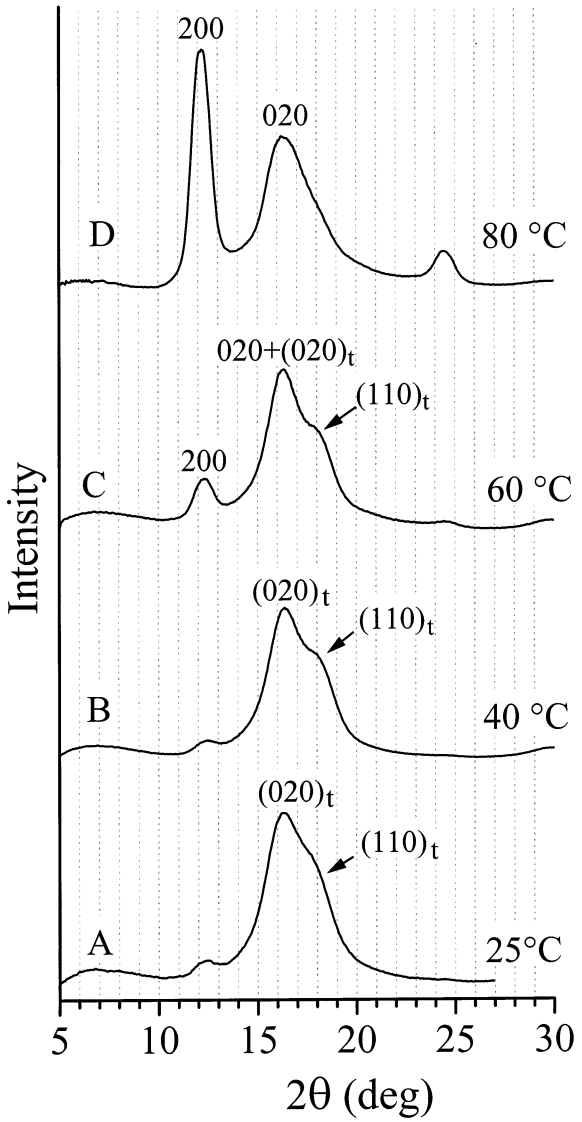

Figure 6. X-ray diffraction profiles read along the equatorial lines of the X-ray fiber diffraction patterns of Figures 2A−5A for s-PP fibers stretched at 25 °C (A), 40 °C (B), 60 °C (C), and 80 °C (D), up to 600% elongation and kept in tension. The Miller indices $(020)_t$ and $(110)_t$ indicate reflections of the *trans*-planar form III of s-PP, while the indices 200 and 020 indicate reflections at $2\theta = 12.2°$ and 16°, respectively, of the helical form I of s-PP.

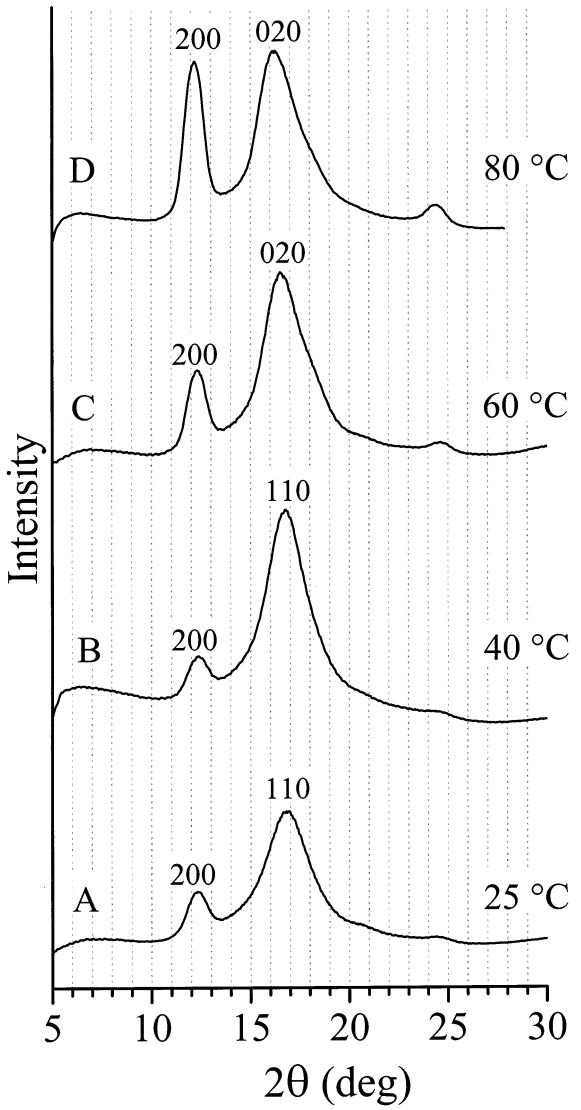

Figure 7. X-ray diffraction profiles read along the equatorial lines of the X-ray fiber diffraction patterns of Figures 2B−5B for s-PP fibers stretched at 25 °C (A), 40 °C (B), 60 °C (C), and 80 °C (D), up to 600% elongation and after the release of the tension at room temperature. The Miller indices 200 indicates the reflection of the both helical forms (forms I and II) of s-PP, while the indices 020 and 110 indicate reflections at $2\theta = 16°$ and 17° of the helical antichiral form I and isochiral form II, respectively.

pattern of the fiber stretched at 80 °C (Figures 5A and 6D) shows only spots on the layer lines of the helical form and the equatorial 200 and 020 reflections at $2\theta = 12.2°$ and 16°, respectively, typical of form I.

In the equatorial diffraction profiles of the fibers obtained at low stretching temperatures of Figure 6A,B, the peaks at $2\theta = 16°$ correspond to the $(020)_t$ reflection of the *trans*-planar form III. With increasing the stretching temperature, besides the increase of the intensity of the 200 reflection at $2\theta = 12.2°$, also an increase of the diffraction peak at $2\theta = 16°$ is clearly observed (Figure 6C,D). This indicates that the helical polymorphic form which develops at high stretching temperatures is the antichiral form I, characterized by the 020 reflection at $2\theta = 16°$. At 80 °C only the 020 reflection of the helical form I is present (Figure 6D).

After releasing the tension in the stretched fibers the orientation of the crystals is preserved. The degree of orientation has been evaluated from the X-ray fiber diffraction patterns of Figures 2−5 as the half-height width of the peaks obtained in the azimuthal scans of the reflections at $2\theta = 12.2°$ for the fibers in the helical form and at 16° for the fibers in the *trans*-planar form III. The fibers stretched at low temperatures (25 and 40 °C), which are in the *trans*-planar form III, show a degree of orientation of 6°. The fibers stretched at 60 and 80 °C, which are in the helical form, show degrees of orientation of 12° and 7°, respectively. After the release of the tension a decrease of orientation is observed in the case of the fibers stretched at 25 and 40 °C, the degrees of orientation being 20° and 10°, respectively (Figures 2B and 3B), whereas the same high orientation is maintained in the fibers stretched at 60 and 80 °C (Figures 4B and 5B).

It is apparent from Figures 2 and 3 that the *trans*-planar form III, obtained in the fibers stretched at low temperatures (25 and 40 °C) (Figures 2A, 3A, and 6A,B), transforms into the helical form by releasing the ten-

sion, as indicated by the appearance in the X-ray diffraction patterns of Figures 2B and 3B of the 200 reflection at $2\theta = 12.2°$ (see also the equatorial diffraction profiles of Figure 7A,B) and the 111 reflection on the first layer line corresponding to the helical periodicity of 7.4 Å. The presence of the 110 reflection at $2\theta = 17°$ in the patterns of Figures 2B, 3B, and 7A,B indicates that the helical polymorphic form which is present in these stress-relaxed fibers is the isochiral form II. A small amount of ordered domains with chains in *trans*-planar conformation is present as indicated by the presence in the patterns of Figures 2B and 3B of weak diffraction spots on the layer line corresponding to the *trans*-planar periodicity of 5.1 Å.

As discussed above, the fibers stretched at higher temperatures are basically in the helical form I, and the amount of *trans*-planar form III progressively decreases with increasing the temperature (Figures 4A, 5A, and 6C,D). After releasing the tension in the fibers stretched at 60 and 80 °C, a high orientation of the crystals is still present and the fibers remain essentially in the helical form I, as indicated by the presence of the strong 200 and 020 reflections at $2\theta = 12.2°$ and 16°, respectively, in the X-ray diffraction patterns of Figures 4B, 5B, and 7C,D. The presence of the 211 reflection on the first layer line of the X-ray diffraction patterns of Figure 5A,B indicates the presence of more ordered crystals of form I, characterized by a higher degree of order in the regular alternation of right- and left-handed helices along the *a* and *b* axis of the orthorhombic unit cell (Figure 1A). The formation of these ordered crystals competes with the formation of crystals in the *trans*-planar form III during the stretching of unoriented sPP films at temperatures higher than 60 °C. Therefore, stretching at temperatures higher than 60 °C does not increase the relative amount of the crystalline phase but stabilizes the helical polymorph, increasing the amount of crystals in ordered modifications of form I, which are stable even after releasing the tension. This leads, as we shall see in the next section, to more rigid (and less elastic) materials.

The different polymorphic behavior of fibers relaxed after the stretching at different temperatures is clearly shown in Figure 7. It is apparent that the peak at $2\theta = 17°$, corresponding to the 110 reflection of form II, present in the X-ray diffraction profiles of fibers relaxed after the stretching at 25 and 40 °C (Figure 7, A and B, respectively), moves at $2\theta = 16°$, corresponding to the 020 reflection of form I, with increasing the stretching temperature (Figure 7C,D). The isochiral helical form II, obtained upon the release of the tension in fibers stretched at low temperatures, does not form in fibers stretched at higher temperatures. High stretching temperatures prevent not only the formation of the *trans*-planar form III of s-PP but even that of the isochiral helical form II.

These data indicate that the formation of the isochiral helical form II (Figure 1B) of s-PP is strictly related to that of the *trans*-planar form III (Figure 1C). The isochiral helical form II can be obtained only from stretched fibers initially in the *trans*-planar form III upon the release of the tension.[12,13] Only when the *trans*-planar form III can be obtained, for instance by stretching at low temperatures (Figures 2A, 3A, and 6A,B) can the isochiral helical form II be obtained by releasing the tension (Figures 2B, 3B, and 7A,B). At high stretching temperatures the *trans*-planar form III cannot be obtained, and as a consequence, the isochiral helical form II does not form anymore. These data are in agreement with the results recently reported on copolymers of s-PP with 1-butene.[21] Stretched fibers of copolymers with small content of 1-butene (1−2 mol %) are in the *trans*-planar form III of s-PP, which transforms into the isochiral helical form II upon the release of the tension.[21] With increasing 1-butene content only the antichiral helical form I of s-PP is observed in the stretched fibers of the copolymers as well as upon the release of the tension. The presence of 1-butene units, for contents higher than 4 mol %, prevents the formation of the *trans*-planar form III of s-PP by stretching, and the isochiral helical form II does not form any more.[21]

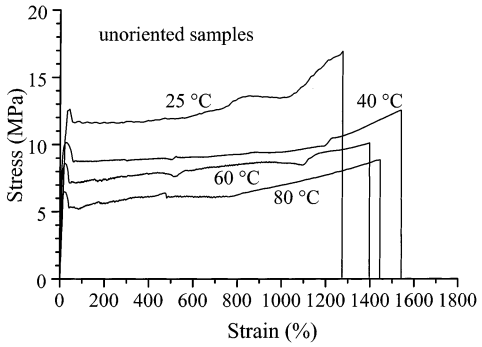

Figure 8. Stress−strain curves of unoriented compression molded films of s-PP stretched at the indicated temperatures (experiments 1−4 in Table 1).

Therefore, anytime the formation of the *trans*-planar form III of s-PP is prevented, like in the presence of butene comonomeric units or by stretching at high temperatures, the isochiral helical form II is not observed. The metastable isochiral form II of s-PP can be obtained, at atmospheric pressure, only starting from the *trans*-planar form III by a spontaneous transformation when the tension in stretched fibers is removed.[12,13] This transformation is a crystal−crystal transition as demonstrated by time-resolved diffraction experiments with synchrotron radiation.[22] As discussed in our recent paper,[23] this crystal−crystal transformation, involving a conformational transition from *trans*-planar to helical conformation, is a cooperative process imposed by steric constraints. The cooperativity induces the formation of helical chains having the same chirality, which pack forming the metastable isochiral C-centered form II of s-PP (Figure 1B), even though the antichiral helical form I (Figure 1A) of s-PP is more stable. The results of the stretching of s-PP at different temperatures confirm that the helical form II of s-PP can be obtained only through this cooperative conformational transition. When the *trans*-planar form III is absent, the most stable antichiral form I of s-PP forms in the fiber samples under any conditions.

Mechanical Properties. The stress−strain curves of unoriented compression-molded films of s-PP stretched at different temperatures (experiments 1−4 in Table 1) are reported in Figure 8. The mechanical properties (i.e., Young's modulus, stress and strain at break, stress and strain at yield point, and tension set at break) measured at different temperatures are reported in Table 2 and Figure 9. It is apparent that with increasing temperature the values of the modulus and the stress at break and at the yield point decrease, whereas the values of the strain at break remain nearly constant. The values of the tension set have been measured at room temper-

Table 2. Elastic Modulus (E), Stress (σ_b) and Strain (ϵ_b) at Break, Stress (σ_y) and Strain (ϵ_y) at the Yield Point, and Tension Set at Break (t_b) for Unoriented Compression-Molded Films of s-PP Stretched at Different Temperatures

T (°C)	E (MPa)	σ_b (MPa)	ϵ_b (%)	σ_y (MPa)	ϵ_y (%)	t_b (%)
25	134 ± 5	17 ± 1	1335 ± 30	13 ± 1	30 ± 4	625
40	131 ± 11	13 ± 1	1538 ± 29	10 ± 1	28 ± 1	728
60	127 ± 5	10 ± 1	1380 ± 28	8 ± 1	21 ± 2	621
80	72 ± 5	9 ± 1	1446 ± 63	7 ± 1	19 ± 1	688

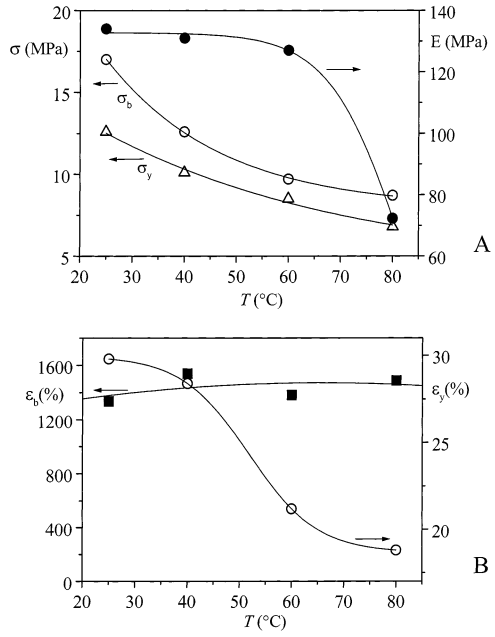

Figure 9. (A) Values of the Young's modulus E (●), stress at the yield point σ_y (△), and stress at break σ_b (○) as a function of the stretching temperature. (B) Values of the strain at the yield point ϵ_y (○) and strain at break ϵ_b (■) as a function of the stretching temperature.

Table 3. Values of the Tension Set ($t_s(\epsilon)$) and the Elastic Recovery ($r(\epsilon)$) for Unoriented Compression-Molded Films of s-PP of Initial Length L_0, Stretched up to 600% Elongation (Final Length $L_f = 7L_0$) at Different Temperatures (Experiments 1a−4a in Table 1), Kept in Tension for 2 days at Room Temperature, and Then Relaxed by Releasing the Tension (Experiments 1b−4b in Table 1)

T (°C)	$t_s(\epsilon)$ (%)	$r(\epsilon)$ (%)
25	314	69
40	355	54
60	380	46
80	527	14

ature also for unoriented specimens stretched at different temperatures at 600% elongation (experiments 1a−4a in Table 1). The values of the tension set and the elastic recovery are reported in Table 3. The high values of the tension set (Tables 2 and 3) indicate that the samples, when not previously oriented, show only fair or very poor elastic properties at any temperature. With increasing the stretching temperature the values of the tension set increase, in particular the sample stretched at 80 °C at 600% elongation (experiment 4a in Table 1) presents a tension set of 527% (Table 3), indicating that the sample undergoes only a plastic deformation and does not present any elastic recovery at room temperature after the plastic deformation.[13]

These results are possibly related to the structural analysis reported above. With increasing the stretching temperature the *trans*-planar form III does not form,

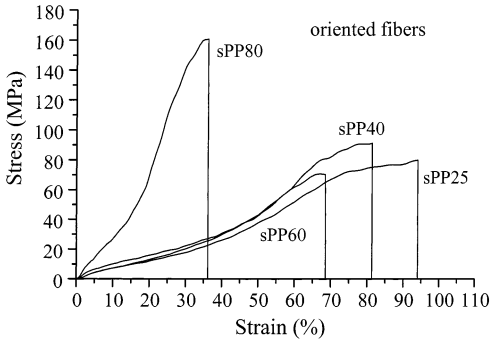

Figure 10. Stress−strain curves recorded at room temperature of strained and stress-relaxed s-PP fibers (experiments 1c−4c in Table 1). The fibers sPP25, sPP40, sPP60, and sPP80 are stress-relaxed fibers obtained by stretching compression-molded films of s-PP up to 600% elongation at 25, 40, 60, and 80 °C, respectively, keeping the fiber under tension for 2 days at room temperature and then removing the tension.

Table 4. Elastic Modulus (E), Stress (σ_b) and Strain (ϵ_b) at Break (Evaluated from Experiments 1c−4c of Table 1), Tension Set ($t_s(\epsilon)$), and Elastic Recovery ($r(\epsilon)$) at the Elongation (ϵ, %) (Evaluated from Experiments 1d,e−4d,e of Table 1) for Strained and Stress-Relaxed s-PP Fibers

sample	E (MPa)	σ_b (MPa)	ϵ_b (%)	$t_s(\epsilon)^a$ (%)	$r(\epsilon)^a$ (%)
sPP25	125 ± 6	80	94	8	56
sPP40	122 ± 13	90	81	8	43
sPP60	120 ± 5	70	68	4	40
sPP80	194 ± 5	161	36		

[a] The tension set $t_s(\epsilon)$ and the elastic recovery $r(\epsilon)$ have been evaluated by stretching the fibers of initial length L_r up to the final length $L_f = 7L_0$ (experiments 1d−4d in Table 1), that is, up to the elongation $\epsilon = [(7L_0 - L_r)/L_r] \times 100$; $t_s(\epsilon) = [(L_r' - L_r)/L_r] \times 100$, and $r(\epsilon) = [(7L_0 - L_r')/L_r'] \times 100$, where L_r' is the final length after the release of the tension (experiments 1e−4e in Table 1).

and fibers essentially in the helical form I are obtained (Figures 5A and 6D). After releasing the tension at room temperature no structural transition occurs (Figures 5B and 7D), the fibers remains in the helical form I, and, correspondingly, no elastic recovery is observed. Since the crystallinity does not change significantly with the stretching temperature, this indicates that the elastic behavior of s-PP is possibly related to the reversible structural transition occurring during the stretching and releasing of the tension.

The mechanical analysis has been performed also on oriented stress-relaxed fibers. These stress-relaxed fibers have been prepared by stretching compression-molded films of s-PP of initial length L_0 at different temperatures up to 600% elongation (the final length L_f being $7L_0$, experiments 1a−4a in Table 1), keeping the fibers under tension for 2 days at room temperature, and then removing the tension at room temperature (samples sPP25, sPP40, sPP60, and sPP80 for stretching temperatures of 25, 40, 60, and 80 °C, experiments 1b−4b in Table 1). After the relaxation, the final lengths of these fibers are $L_r = L_0(t_s/100) + L_0$, where t_s is the value of the tension set reported in Table 3. The X-ray fiber diffraction patterns of such stress-relaxed fibers, previously stretched at $\epsilon = 600\%$ ($L_f = 7L_0$), have been already shown in Figures 2B−5B and 7. The stress−strain curves of these fibers measured at room temperature are reported in Figure 10 (experiments 1c−4c in Table 1). The mechanical properties of the four fibers are reported in Table 4.

As already shown in ref 13, the mechanical properties of oriented stress-relaxed fibers of s-PP are very differ-

ent from those of the unoriented compression-molded films. It is apparent from Figure 10 that the values of the stress at a given elongation are higher than those measured on not previously oriented specimens (Figure 8). Moreover, with increasing the stretching temperature used to prepare the fibers, the strain at break decreases, whereas the stress at break and the elastic modulus remain nearly constant for the first three samples and increase for the sample sPP80 (Table 4). This increased rigidity of the fiber sPP80 cannot be due to a higher crystallinity of the fiber stretched at 80 °C, because, as already discussed, the degree of crystallinity remains nearly constant in this small range of stretching temperatures. As discussed in the previous section, the stress-relaxed fibers sPP25 and sPP40 are crystallized in the isochiral form II of sPP, whereas the stress-relaxed fiber sPP80 is crystallized in well-oriented and more ordered crystals of the helical form I, characterized by higher degree of order in the regular alternation of right- and left-handed helices along the axes of the unit cell. The presence of more oriented and more ordered crystals of form I in the fiber sPP80 probably accounts for the increased rigidity of the sample.

The values of the tension set $t_s(\epsilon)$ and the elastic recovery $r(\epsilon)$ of the four fibers, reported in Table 4, have been measured by stretching at room temperature the fibers having the new initial length L_r, up to the final length $L_f = 7L_0$ (experiments 1d−4d in Table 1), that is, up to an elongation $\epsilon = [(L_f - L_r)/L_r] \times 100$ (corresponding to the elastic recovery reported in Table 3, i.e., $\epsilon = 69$, 54, and 46% for sPP25, sPP40, and sPP60 fibers, respectively), keeping the fibers in tension for 10 min, then removing the tension, and measuring the final length of the relaxed fibers after 10 min (experiments 1e−4e in Table 1). These values of the elongation ϵ have been chosen to reduce the possibility of new plastic deformation of the fibers during the measure of the elastic recovery. Since the fiber stretched at 80 °C experiences a very small elastic recovery after removing the tension from 600% elongation ($r(600) = 14\%$, $t_s(600) = 527\%$, Table 3), the stress-relaxed sPP80 fiber, stretched again at room temperature up to $L_f = 7L_0$ (experiment 4d in Table 1), undergoes only a very small deformation $\epsilon = 14\%$. For this fiber the value of the tension set after this small deformation of 14% is meaningless (not reported in Table 4) because the fiber has been stretched and relaxed inside its elastic deformation range. For the other three stress-relaxed fibers the low values of the tension set (Table 4), and the shape of the stress−strain curves up to the break (Figure 10), indicate that the stress-relaxed fibers show a good elastic behavior (tension set lower than 10%)[24] regardless of the temperature at which the samples have been previously stretched.

To quantify the elastic properties of the s-PP fibers, hysteresis cycles have been performed at room temperature on the oriented stress-relaxed fibers. The hysteresis cycles, composed of the stress−strain curves measured at room temperature during the stretching, immediately followed by the curves measured during the relaxation at controlled rate, for the sPP25, sPP40, sPP60, and sPP80 fibers, are reported in Figure 11. In these cycles, stress-relaxed oriented fibers having new initial length L_r are stretched up to the final length $L_f = 7L_0$ (experiments 1d−4d in Table 1), that is, also in this case, up to a maximum strain $\epsilon_{max} = [(L_f - L_r)/L_r] \times 100$, numerically coincident with the elastic recovery reported in Table 3 ($\epsilon_{max} = 69$, 54, 46, and 14% for the sPP25, sPP40, sPP60, and sPP80 fibers, respectively). As discussed before, this choice of the maximum strain in the hysteresis cycle is due to the need to reduce to a minimum a new plastic deformation of the fibers during the first hysteresis cycle.

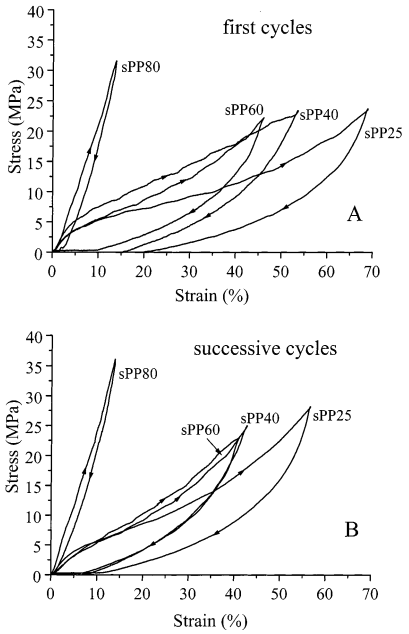

Figure 11. Stress−strain hysteresis cycles recorded at room temperature, composed of the stretching and relaxation (at controlled rate) steps according to the direction of the arrows, for strained and stress-relaxed sPP fibers. sPP25, sPP40, sPP60, and sPP80 fibers are stress-relaxed from fibers stretched up to 600% elongation at 25, 40, 60, and 80 °C, respectively. In the hysteresis cycles the stretching steps are performed stretching the fibers up to the final length $L_f = 7L_0$, that is, up to a maximum elongation $\epsilon_{max} = [(L_f - L_r)/L_r] \times 100$. (A) First cycles; (B) curves averaged for at least four cycles successive to the first one.

The first hysteresis cycles of the stress-relaxed fibers are reported in Figure 11A, whereas the successive cycles, measured after the first one, are reported in Figure 11B. Each cycle is performed after 10 min the end of the previous cycle. Successive hysteresis cycles, measured after the first one, are all nearly coincident, indicating a tension set close to zero. All the stress-relaxed fibers recover almost completely the initial dimensions.

The oriented stress-relaxed fibers of s-PP present good elastic behavior at room temperature regardless of the stretching temperature at which they have been prepared. It is worth noting that the hysteresis cycles of the fiber sPP80 can be performed only in a very small deformation range (0−14%), because, as discussed above, the fiber obtained by stretching the unoriented specimens at 80°C are poorly elastic (the elastic recovery r is only 14%, see Table 3). In this small deformation range the fiber shows a meaningless elastic behavior (the tension set is close to zero in successive cycles, Figure 11), because the fiber is, in both the strained and relaxed state, close to its possible maximum deformation.

As shown by the X-ray diffraction patterns of Figures 2B−5B and 7, all the stress-relaxed fibers are basically in the helical polymorphic forms of s-PP. The fibers sPP25 and sPP40, stretched at low temperatures (25 and 40 °C, respectively), and then relaxed from the

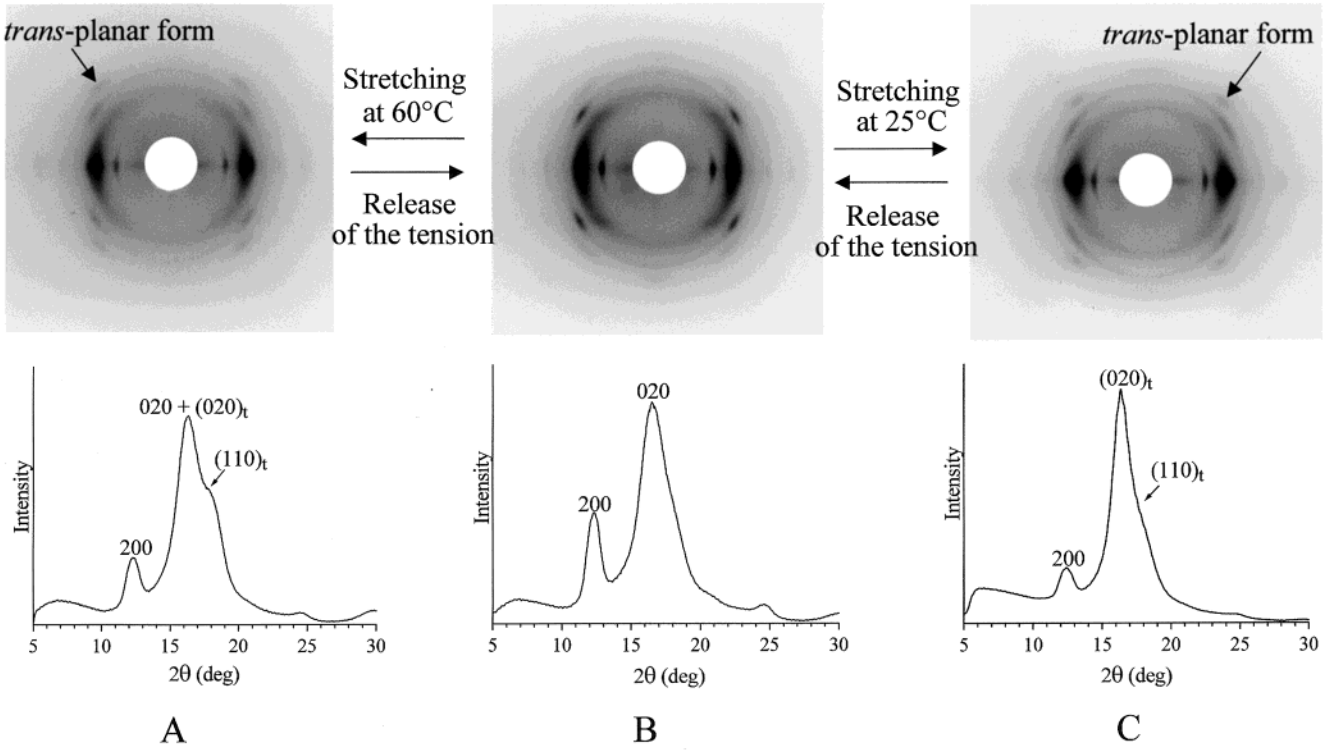

Figure 12. X-ray fiber diffraction patterns and corresponding profiles read along the equatorial lines of the fiber obtained by stretching at 60 °C compression-molded films at 600% elongation (experiment 3a in Table 1), keeping the fiber under tension (A), after removing the tension (experiment 3b in Table 1) (B) and after a new stretching at room temperature up to the final length $L_f = 7L_0$ (experiment 3d in Table 1), keeping the fiber in tension (C). The Miller indices $(020)_t$ and $(110)_t$ indicate reflections of the *trans*-planar form III of s-PP, while the indices 200 and 020 indicate reflections at $2\theta = 12.2°$ and 16° of the helical form of s-PP. The fibers in (A) and (C) are in mixtures of the *trans*-planar form and helical form I (the latter with lower amount), whereas the fiber in (B) is basically in the helical form I with a small amount of the *trans*-planar form III.

tension are in the isochiral form II (Figures 2B, 3B, and 7A,B), whereas the fibers sPP60 and sPP80, stretched at high temperatures (60 and 80 °C, respectively), are in the antichiral form I (Figures 4B, 5B, and 7C,D). When the stress-relaxed sPP25, sPP40, and sPP60 fibers are stretched again at room temperature (experiments 1d, 2d, and 3d in Table 1), like in the hysteresis experiments of Figure 11, both the helical forms, form I or form II, transform, at least in part, into the *trans*-planar form III. For instance, in Figure 2 it was already shown that the helical form II (Figure 2B) transforms into the *trans*-planar form by stretching at room temperature (Figure 2A). Moreover, the X-ray diffraction pattern of the fiber sPP60 stretched again at room temperature up to a final length $L_f = 7L_0$ (experiment 3d in Table 1), reported in Figure 12C, presents the $(020)_t$ and $(110)_t$ reflections and spots on the first layer line typical of the *trans*-planar form III, while the intensity of the 200 reflection at $2\theta = 12.2°$ of the helical form is reduced with respect to that in the pattern of the stress-relaxed fiber (Figure 12B). This indicates that the helical form I (Figure 12B) partially transforms in the *trans*-planar form by stretching at room temperature (Figure 12C). Upon the release of the tension the *trans*-planar form III transforms at room temperature again into the helical form (Figures 2B and 12B). In this condition a good elastic behavior is observed (Figure 11). These data indicate that the occurrence of the structural transition plays a significant role in the elastic behavior of s-PP fibers.

In the case of the stress-relaxed sPP80 fiber, the X-ray diffraction pattern of the fiber stretched again at room temperature up to the final length $L_f = 7L_0$ ($\epsilon_{max} = 14\%$) is very similar to the pattern of the relaxed fiber of Figure 5B; i.e., the fiber remains in the helical form I upon stretching. Therefore, for this fiber the stretching at room temperature does not induce transformation of the helical form into the *trans*-planar form, probably because the fiber has almost achieved its maximum deformation and the further strain of only 14% is not enough for the structural transition. In the hysteresis cycle of the fiber sPP80 of Figure 11 there is no contribution of the reversible transition, and a meaningless elastic behavior is observed, because the fiber is stretched inside its elastic deformation range.

To verify whether the elastic properties of the stress-relaxed fibers are maintained even at high temperatures, mechanical tests have been performed at 60 and 80 °C on fibers of s-PP prepared by stretching at room temperature up to 600% elongation and then removing the tension (experiments 5 and 6 in Table 1). The hysteresis cycles of such fibers, performed at 60 and 80 °C, are reported in Figure 13, A and B, respectively. A different behavior with respect to the hysteresis cycles at room temperature (Figure 11) is apparent. At 60 °C very different stretching and relaxing curves (no longer superimposed) are obtained in the successive cycles. This is due to the fact that after each relaxation of the fiber there is no recovery of the initial dimension. A residual deformation of the fiber is instead observed between successive cycles (the tension set is always very high, Figure 13A), and the possible maximum strain achieved in the successive stretching curves is progressively reduced. In other words, the fiber shows bad elastic properties at 60 °C.

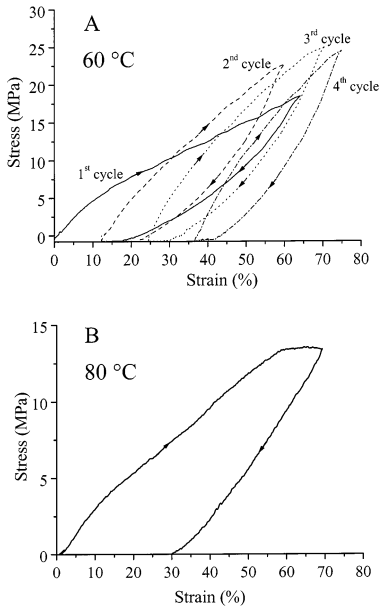

Figure 13. Stress−strain hysteresis cycles performed at 60 °C (A) and 80 °C (B) for stress-relaxed fibers of s-PP of initial length L_r (experiments 5 and 6 in Table 1), prepared by stretching at room temperature compression-molded films of length L_0 up to the final length $L_f = 7L_0$ (600% elongation) and then removing the tension. In the hysteresis cycles the stretching steps are performed stretching the fibers up to the final length $L_f = 7L_0$, that is, up to a maximum elongation $\epsilon_{max} = [(L_f - L_r)/L_r] \times 100$.

In the hysteresis cycle at 80 °C (Figure 13B) a larger residual deformation of the fiber is observed after the relaxing curve. The fiber does not recover the initial dimension upon relaxation, and after the first cycle, shown in Figure 13B, the fiber cannot be stretched again; it breaks immediately after a small strain, its maximum possible deformation being already achieved.

Therefore, at high temperatures s-PP fibers do not show elastic behavior. This result may be possibly related to the structural analysis reported in the previous section. Stress-relaxed sPP fibers are generally in one of the two helical polymorphic forms (form I or form II) depending on the previous history (Figures 2B−5B). When the fibers are prepared by stretching at room temperature compression-molded films and then removing the tension, they are in the isochiral form II (Figures 2B, 3B, and 7A,B). When the stretching temperature is higher (60 or 80 °C), they are in the antichiral form I (Figures 4B, 5B, and 7C,D). Whichever the helical polymorphic form, when such fibers are stretched again at high temperatures they do not transform into the *trans*-planar form III but remain in the helical form (Figures 4A, 5A, and 6C,D). The helical form II probably only transforms in part into the antichiral form I[10] because of the annealing. Therefore, in the stretching and relaxing cycles at high temperatures (Figure 13) no reversible structural transition between the helical and the *trans*-planar forms occurs. Correspondingly, no elastic behavior is observed.

These data indicate that, when the *trans*-planar form is obtained by stretching, for instance at room temperature, the fibers show elastic behavior,[13] whereas when the formation of the *trans*-planar form is prevented, for instance by stretching at high temperatures, the elastic properties are lost. The formation of the metastable *trans*-planar form and its transformation upon relaxation of the fibers seem to be an important factor possibly related to the origin of the elasticity of s-PP.

The elastic properties of s-PP have been also checked on fibers annealed at high temperatures. Annealing of s-PP fibers in the *trans*-planar form III or in the isochiral form II produces a transformation into the stable helical form I, and fibers with a mixture of crystals of form I and form II are generally obtained.[10] The stress-relaxed fiber sPP25, prepared by stretching at 25 °C compression-molded film up to 600% elongation ($L_f = 7L_0$, experiment 1a in Table 1) (Figure 2A) and removing the tension (experiment 1b in Table 1), is in the isochiral helical form II (Figure 2B), which transforms into the *trans*-planar form upon successive stretching (Figure 2). This fiber has been subjected to successive stretching and relaxing cycles between the final length $7L_0$ and the relaxed length L_r. The tension set in the successive cycles is always very close to zero, indicating a good elastic behavior for this fiber. As shown in Figure 2, during these cycles the *trans*-planar form and the helical form II transform each other reversibly. After the fifth stretching cycle, the stretched fiber kept at $L_f = 7L_0$ (hence in the *trans*-planar form III, Figure 14A) has been annealed at 95 °C for 40 min, keeping the fiber under tension (experiment 7 in Table 1). The X-ray diffraction pattern of the annealed fiber is reported in Figure 14B. It is apparent that the *trans*-planar form transforms into the helical form I upon annealing, as indicated by the presence of the 200 and 020 reflections at $2\theta = 12.2°$ and 16°, respectively, of form I. Then, the tension has been removed, and the tension set has been measured after the relaxation of the fiber (experiment 7a in Table 1). The X-ray diffraction pattern of the fiber after removing the tension, reported in Figure 14C, is very similar to that of Figure 14B and indicates that the fiber remains in the helical form I. A value of the tension set of 31% is obtained (the length of the relaxed fiber being $L_{ra} = 1.31L_r$). The value of the tension set, higher than that of the unannealed sPP25 fiber, indicates that for the annealed fiber only a partial recovery of the initial dimension occurs. This experiments provides another evidence that, when the formation of the *trans*-planar form and the occurrence of the structural transition are prevented, the elastic properties are partially lost.

The stress-relaxed annealed fiber, having a new length $L_{ra} = 1.31L_r$, has been stretched again up to the final length $L_f = 9L_0$ (experiment 7b in Table 1). The helical form transforms again partially into the *trans*-planar form III by stretching, as indicated in Figure 14D by the decrease of the 200 reflection at $2\theta = 12.2°$. Upon the release of the tension (experiment 7c in Table 1), the *trans*-planar form transforms again into the helical form (Figure 14E), and a recovery of the dimension from the length $9L_0$ to the initial length L_{ra} is observed, the tension set being nearly zero. This experiment also shows that when the *trans*-planar form III forms in stretched fibers a nearly total recovery of the dimension is observed upon the release of the tension, whereas only a partial recovery occurs when the stretched fibers are in the helical form, and no structural transition occurs upon the release of the tension.

These data indicate that the elastic property of s-PP depends on the crystalline form in the stretched fiber and, therefore, that the elastic recovery is, at least in part, linked to the enthalpy gain achieved when the fibers are relaxed from the tension. Since a partial

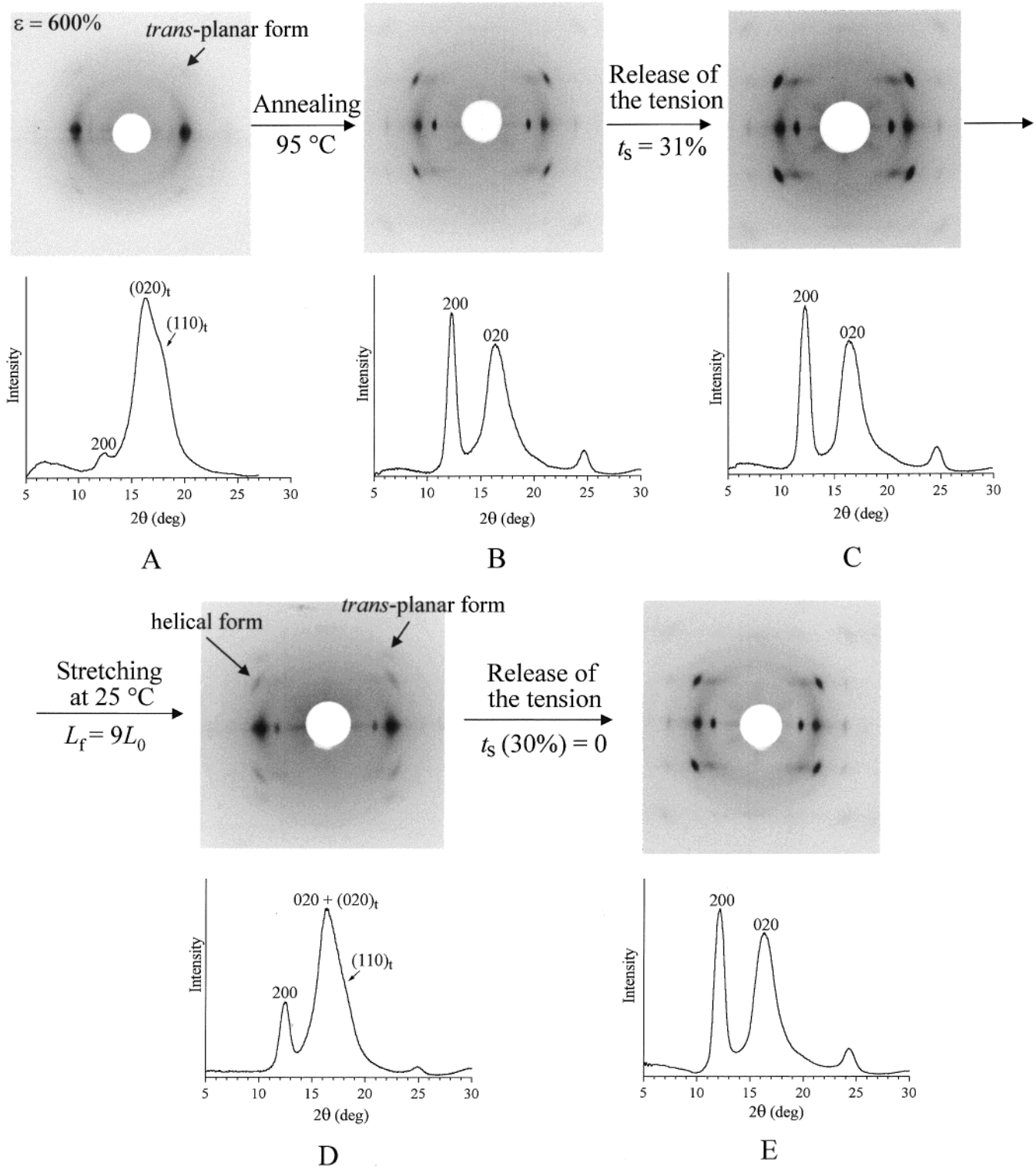

Figure 14. X-ray fiber diffraction patterns and corresponding equatorial profiles of the sPP25 fiber after five cycles of stretching and relaxation, stretched up to the final length $L_f = 7L_0$ and kept in tension (A), then annealed at 95 °C for 40 min and kept in tension (experiment 7 in Table 1) (B), after the release of the tension (experiment 7a in Table 1) (C), after a new stretching up to the final length $L_f = 9L_0$ (experiment 7b in Table 1) (D), and after removing the tension (experiment 7c in Table 1) (E). The $(020)_t$ and $(110)_t$ reflections of the *trans*-planar form III and the 200 and 020 reflections of the helical form I of s-PP are also shown. The fiber in (A) is in the *trans*-planar form III, the fibers in (B), (C), and (E) are in the helical form I, and the fiber in (D) is in a mixture of *trans*-planar and helical forms.

recovery of the fiber dimension is observed also when no structural transition occurs, the amorphous phase may play an important role as well, like in conventional elastomers.[19,20] The chains in the amorphous fraction are of course involved in the stretching and relaxation process. They are probably well-oriented and in extended conformation in the stretched state and experience a reversible conformational transition between the disordered (coil) and extended conformations when the fibers are repeatedly stretched and relaxed. These chains are also highly entangled, because of the high molecular weight of s-PP, and connect different crystals

where a structural transition generally occurs during the mechanical cycles. When the tension is removed, either the enthalpic factor, due to the structural transition in the crystalline regions, or an entropic factor, due to the return of the entangled and extended amorphous chains to the unstrained conformationally disordered state, contributes to the elastic recovery of the fibers.

The discrimination between the relative contributions of the enthalpic and entropic factors is an important issue, which, at the moment, is difficult to address. The loss of the elastic properties at high temperatures could be due to the decrease of the amount of amorphous chains, which connect the crystals and act as springs, as a consequence of a possible crystallization induced by the strain and annealing. However, our X-ray diffraction data have shown that the degrees of crystallinity and orientation of the s-PP fibers stretched at different temperatures, and of the relaxed fibers after removing the tension, are nearly the same, and no significant further crystallization occurs. (The starting compression-molded film used to prepare the fibers already presents a high crystallinity because of the slow crystallization from the melt). Moreover, the data of Figure 14 have shown that the perfect elastic behavior of the stress-relaxed fiber sPP25 (stretched at 25 °C at 600% elongation and then relaxed) is lost after annealing at 95 °C (the tension set being 31%, Figure 14B,C), but the same annealed fiber presents again elastic property if it is stretched again at room temperature (tension set = 0, Figure 14D,E). In this condition, even though a certain decrease of the amount of amorphous tie-chains acting as springs is possible, as a consequence of the annealing, the fiber still shows elastic behavior. Fibers annealed at high temperatures may show (Figure 14D,E) or not (Figure 14B,C) elastic properties depending on the occurrence of the crystalline structural transition. If the structural transition occurs during the stretching and the successive relaxation, nearly total elastic recovery is observed (Figure 14D,E). However, since a partial recovery has been observed after removing the tension of the annealed fiber, even in the absence of structural crystalline transition (Figure 14B,C), the entropic contribution of the amorphous phase is also important.

It is worth noting, in addition, that we have demonstrated, through time-resolved X-ray diffraction experiments with synchrotron radiation performed during the stretching and the relaxation of s-PP fibers, that the reversible structural transition between the *trans*-planar form III and the helical form is a crystal−crystal transition,[22] and no evidence of the occurrence of melting and recrystallization phenomena during the stretching and the relaxation has been found. This supports the hypothesis of the presence of an elthalpy gain produced during the relaxation process, associated with the entropic factor due to the conformational transition of the amorphous chains.

As discussed in our previous paper,[13] the elastic properties of s-PP depends on the microstructure of the sample and, in particular, on the stereoregularity. We have shown that the lower the degree of stereoregularity, the more difficult is the formation of the *trans*-planar form III by stretching. It is, therefore, expected that the enthalpic contribution to the elasticity, due to the structural transition, is more important in highly stereoregular samples and less important in low stereoregular samples.

Conclusion

When s-PP samples are stretched at room temperature, the *trans*-planar form III is generally obtained in the strained fibers. The *trans*-planar form transforms into the isochiral helical form II upon the release of the tension. Stretching at higher temperatures (80 °C) prevents the formation of the *trans*-planar form III, and fibers in the stable antichiral helical form I are obtained. In this case no structural transition is observed when the tension is removed. These data confirm that the isochiral form II can be obtained only starting from stretched fibers in the *trans*-planar form III through a solid−solid transition occurring when the tension is released and involving a cooperative process, which produces helical chains having the same chirality.

Fibers of s-PP stretched at room temperature show good elastic properties, which are lost at higher temperatures. When stretched fibers are in the metastable *trans*-planar form III, a nearly total recovery of the initial dimension occurs when the tension is removed. Instead, when stretched fibers are in the stable helical form I, like for instance in fibers stretched at high temperatures or in annealed fibers, and no structural transition occurs upon the release of the tension, only a partial recovery is observed. These data indicate that both the metastability of the *trans*-planar form III, which transforms into the stable helical form when the tension is relaxed, and the conformational transition of the chains in the amorphous phase play key roles in the elastic behavior of s-PP. The structural transition occurring in the crystalline regions, due to the metastability of the *trans*-planar form in the unstrained state, produces an enthalpy gain when the tension is removed, which is in part responsible for the elastic recovery of the fibers. On the other hand, chains belonging to the amorphous phase and connecting the crystalline regions are also involved in the stretching and relaxation process. These chains are probably well-oriented, highly entangled, and in extended conformation in the stretched state and experience a reversible conformational transition between the disordered (coil) and extended conformations when the fibers are repeatedly stretched and relaxed. This entropic factor is probably also involved in the recovery process. The two effects, the enthalpy gain in the crystalline regions and the entropic factor for the amorphous chains, act simultaneously and are, probably, mutually assisted.

It is worth noting that a reversible crystal−crystal phase transition between stretched and relaxed states has been found also in polyethers[25,26] and in some aromatic polyesters.[27,28] In particular, in the case of the poly(trimethylene terephthalate) and poly(tetramethylene terephthalate) also elastic properties have been observed,[28] which have been associated with reversible strains of the crystalline lattices.[27] The diffraction pattern of poly(trimethylene terephthalate) changes, indeed, monotonically with increasing macroscopic strain, suggesting that the lattice responds immediately to the applied stress and deforms like a coiled spring. In the case of poly(tetramethylene terephthalate), the X-ray diffraction pattern changes at high strains, suggesting a definitive change in the crystal structure.[27] In both cases it was concluded that the molecular conformations in both the crystalline and noncrystalline regions play a key role in determining the mechanical behavior of these polymers.[27,28]

Acknowledgment. Financial support of the "Ministero dell'Università e della Ricerca Scientifica e Tecnologica" (PRIN 2000 and Cluster C26) is gratefully acknowledged.

References and Notes

(1) Natta, G.; Corradini, P.; Ganis, P. *Makromol. Chem.* **1960**, *39*, 238.
(2) Corradini, P.; Natta, G.; Ganis, P.; Temussi, P. A. *J. Polym. Sci., Part C* **1967**, *16*, 2477.
(3) Natta, G.; Peraldo, M.; Allegra, G. *Makromol. Chem.* **1964**, *75*, 215.
(4) Lotz, B.; Lovinger, A. J.; Cais, R. E. *Macromolecules* **1988**, *21*, 2375.
(5) Lovinger, A. J.; Lotz, B.; Davis, D. D. *Polymer* **1990**, *31*, 2253.
(6) Lovinger, A. J.; Davis, D. D.; Lotz, B. *Macromolecules* **1991**, *24*, 552.
(7) Lovinger, A. J.; Lotz, B.; Davis, D. D.; Padden, F. J. *Macromolecules* **1993**, *26*, 3494.
(8) Chatani, Y.; Maruyama, H.; Noguchi, K.; Asanuma, T.; Shiomura, T. *J. Polym. Sci., Part C* **1990**, *28*, 393.
(9) Chatani, Y.; Maruyama, H.; Asanuma, T.; Shiomura, T. *J. Polym. Sci., Polym. Phys.* **1991**, *29*, 1649.
(10) De Rosa, C.; Corradini, P. *Macromolecules* **1993**, *26*, 5711.
(11) De Rosa, C.; Auriemma, F.; Vinti, V. *Macromolecules* **1997**, *30*, 4137.
(12) De Rosa, C.; Auriemma, F.; Vinti, V. *Macromolecules* **1998**, *31*, 7430.
(13) Auriemma, F.; Ruiz de Ballesteros, O.; De Rosa, C. *Macromolecules* **2001**, *34*, 4485.
(14) Rastogi, S.; La Camera, D.; van der Burgt, F.; Terry, A. E.; Cheng, S. Z. D. *Macromolecules* **2001**, *34*, 7730.
(15) Auriemma, F.; Born, R.; Spiess, H. W.; De Rosa, C.; Corradini, P. *Macromolecules* **1995**, *28*, 6902.
(16) De Rosa, C.; Auriemma, F.; Vinti, V.; Grassi, A.; Galimberti, M. *Polymer* **1998**, *39*, 6219.
(17) De Rosa, C.; Auriemma, F.; Talarico, G.; Busico, V.; Caporaso, L.; Capitani, D. *Macromolecules* **2001**, *35*, 1314.
(18) De Rosa, C.; Auriemma, F.; Fanelli, E.; Talarico, G.; Capitani, D. *Macromolecules*, in press.
(19) Loos, J.; Schimanki, T. *Polym. Eng. Sci.* **2000**, *40*, 567.
(20) D'Aniello, C.; Guadagno, L.; Naddeo, C.; Vittoria, V. *Macromol. Chem. Rapid Commun.* **2001**, *22*, 104. Guadagno, L.; D'Aniello, C.; Naddeo, C.; Vittoria, V. *Macromolecules* **2001**, *34*, 2512.
(21) De Rosa, C.; Auriemma, F.; Orlando, I.; Talarico, G.; Caporaso, L. *Macromolecules* **2001**, *34*, 1663.
(22) Auriemma, F.; De Rosa, C. Manuscript in preparation.
(23) Lotz, B.; Mathieu, C.; Thierry, A.; Lovinger, A. J.; De Rosa, C.; Ruiz de Ballesteros, O.; Auriemma, F. *Macromolecules* **1998**, *31*, 9253.
(24) Treolar, L. R. G. *The Physics of Rubber Elasticity*; Clarendon Press: Oxford, 1975.
(25) Takahashi, Y.; Sumita, I.; Tadokoro, H. *J. Polym. Sci., Part B* **1973**, *11*, 2113.
(26) Takahashi, Y.; Osaki, Y.; Tadokoro, H. *J. Polym. Sci., Part B* **1981**, *19*, 1153.
(27) Jakeways, R.; Ward, I. M.; Wilding, M. A.; Hall, I. H.; Desborough, I. J.; Pass, M. G. *J. Polym. Sci., Part B* **1975**, *13*, 799.
(28) Ward, I. M.; Wilding, M. A.; Brody, H. *J. Polym. Sci., Part B* **1976**, *14*, 263.

MA020394+